Molecularly based criteria for shear banding in transient flow of entangled polymeric fluids

Mouge Mohagheghi and Bamin Khomami

Phys. Rev. E **93**, 062606 — Published 13 June 2016

DOI: 10.1103/PhysRevE.93.062606

Molecularly Based Criteria for Shear banding in Transient Flow of Entangled Polymeric Fluids

Mouge Mohagheghi and Bamin Khomami*

Material Research and Innovation Laboratory, Department of Chemical and Biomolecular Engineering,
The University Tennessee, Knoxville, TN 37996, USA

Dissipative Particle Dynamics (DPD) simulations of polymeric melts in a start-up of shear flow as a function of ramp-time to its steady state value is studied. Herein, we report for the first time the molecular findings showing the effect of ramp- time on formation of shear banded structures and chain relaxation behavior. Specifically, it is shown that shear banding emerges at rapid start-up, however homogenous shear prevails when the deformation rate ramp time is sufficiently slow. This finding is in full consistency with prior continuum level linear stability analysis of shear banding in startup of shear flows as well as experimental observations of entangled DNA and polymer solutions. Further, for the first time it has been revealed that the ratio of the chain longest orientation relaxation time to that of the time for the imposed deformation rate to reach its steady state value, plays a central role in determining whether local strain inhomogeneities that lead to the formation of shear banded flow structures are created. In addition, we have shown that the gradient of number of entanglements along the velocity gradient direction should reach a critical value for creation of localized strain inhomogeneity. Moreover, the relation between the local process leading to shear banded flows and the relaxation mechanism of the chain is discussed. Overall, a molecular picture for the interrelation between the chain longest orientation and stress relaxation time, local inhomogeneities, and shear banding has been proposed and corroborated with extensive analysis.

PACS numbers: 47.57.Ng, 83.10.RS, 83.50.-v

Corresponding author's email*: bkhomami@utk.edu

I. Introduction

Shear banding occurs in complex fluids due to localized fluid property variations that evolve in time to create two adjoining regions of fluid with a high and low deformation rate. This phenomenon was first experimentally observed in worm-like micelle solutions in the early 1990s [1, 2]. In 2006, shear banding in entangled polymeric fluids was observed experimentally [3] almost two decades after analyses based on the first generation tube-model constitutive equations [4, 5] suggested that banded flow structure are likely to occur in highly entangled polymeric fluids. Specifically, Tapadia and Wang [3] observed a transition between a linear velocity profile to a banded structure in a step-strain start-up flow generated in a cone-and-plate rheometer via Particle Tracking Velocimetry (PTV) when the externally imposed deformation rate was in the stress plateau region of the shear stress versus deformation rate curve. Further, Wang and co-workers documented the existence of this phenomenon (both steady and transient) in different types of shear flows of highly entangled synthetic polymeric fluids (Polybutadiene solutions with molecular weights Mw $\sim 1-2\times10^6$ g/mol) as well as entangled DNA solutions with average number of entanglements per chain greater than forty, i.e., $\langle Z\rangle \geq 40$ [6-10].

Wang and co-workers ascribed the occurrence of shear banding to "cohesive failure" or "elastic yielding" of the highly entangled fluid. On the other hand, Sui and McKenna [11] experiments show that shear banding can also occur in a cone-and-plate rheometer as a result of a hydrodynamic flow instability that is caused by surface distortion, either by edge fracture or by elastic spiral ripples. However, it should be noted that in Wang and co-workers experiments the meniscus was wrapped with a transparent film to avoid edge effects.

The most prevalent yet highly controversial theoretical basis offered to rationalize the occurrence of shear banded flow structures in entangled polymeric fluids is based on the non-monotonic constitutive relation between shear stress and shear rate, as originally proposed by Doi and Edwards [5]. In the DE tube-model, shear stress decreases at shear rates larger than $\dot{\gamma} > \tau_d^{-1}$; it is generally accepted that the flow is unstable in the region where the shear stress is a decreasing function of shear rate and this instability leads to a transition from a unidirectional shear flow to a shear banded flow structure. Recently, linear stability analyses [12-15] based on the most comprehensive tube based constitutive equations including the Roile-Poly model [16], have shown the existence of both steady and transient shear banding. Moreover, Olmsted and coworkers [13-15, 17] have proposed a "mechanic instability" in the region of the constitutive curve with a negative slope that results in formation of steady shear banding in both worm-like micellar and entangled polymeric solutions. On the other hand, Moorcroft and Fielding [18] developed a fluid-universal criterion for the onset of shear banding which depends on the shape of time-dependent rheological response function and is independent of fluid's constitutive law and internal state variables. Cromer et al. [19] have also shown that the steady shear banded flow structures can be obtained with a monotonic constitutive equation in entangled polymeric solutions where the polymer stress and concentration are

coupled. Although nearly identical constitutive relations were used in the aforementioned studies, the discrepancy between their predictions due to the assumed rate of CCR which to a great extent determines the rheological response of the fluid, stress and concentration coupling, monotonic versus non-monotonic flow curves and the choice of perturbation used in the analyses renders their findings regarding the origin of shear banding in entangled polymeric fluids not concrete.

In 1983, the possibility of formation of local inhomogeneities in step-strain startup of unidirectional shear flows of entangled polymeric fluids in the deformation rate regime where a stress overshoot is present was suggested by Marrucci and Grizzuti (MG) [4]. Specifically, they examined the free energy of the system based on the original Doi-Edwards tube-based constitutive equation and identified an inflection point in the free energy at the strain corresponding to the maximum transient stress. Hence, they postulated that the flow is prone to instability in the stress relaxation regime (region where the stress decays from its maximum value to its steady state value; consistent with findings of reference 4 some 30 years later) provided that segmental stress relaxation occurs at a much faster rate than segmental orientation relaxation. Further, they suggested that on a relatively small length scale, the aforementioned elastically driven instability will lead to inhomogeneous deformation in the fluid and hence to shear banding. Morrison and Larson in 1992 [20] assessed the validity of the aforementioned MG postulate in monodisperse and bi-disperse high molecular weight Polystyrene solutions (Mw ~ 2-9 10^6 g/mol) at different concentrations and concluded that the MG postulate to be qualitatively correct in predicting strain inhomogeneities. The concept put forward by MG is further corroborated by experimental results showing the correlation between transient shear banding and existence of stress-overshoot [6, 10]. However, it should be noted that the proposed mechanism by MG for formation of local inhomogeneities in shear flow of entangled polymeric melts is qualitative due to the approximations used in the evaluation of chain segmental orientation relaxation time and the fact that the free energy analysis is based on the DE constitutive equation.

Evidently additional information is required to conclusively develop a molecularly based criterion for the formation of local inhomogeneities and its relation to formation of the incipient shear banded flow structures. Thus, motivated by the MG postulate and findings of Moorcroft and Fielding, we have utilized Dissipative Particle Dynamics (DPD) simulations to investigate the mechanism for the formation of inhomogeneities on a molecular level. Specifically, we have scrutinized the interrelation between chain segmental stress and orientation relaxation times, presence of stress overshoot and formation of shear banded flow structures. To this end, we have performed a series of simulations by varying the time taken for the deformation rate to achieve its steady value.

The aforementioned studies have revealed for the first time that the ratio of the longest chain orientation relaxation time to that of the time for the deformation to reach its steady state value, defined here as "MK" plays a central role in determining whether local inhomogeneities are created in the fluid; a prerequisite for formation of shear banding. Specifically, if MK is greater than one, local inhomogeneity in the entanglement density in the velocity gradient direction is observed and in turn the flow transitions to a shear banded structure. Otherwise, homogenous shear flow prevails. Finally, the local process for the formation of shear banding and its relation to the molecularly universal criterion for occurrence of shear banding is discussed.

II. DPD and Simulation Details

A massively parallel DPD simulation algorithm [21, 22] in conjunction with Lees-Edwards boundary condition [23] has been utilized to study shear banding in planar Couette flow of entangled polymeric melt of N=250 beads/chain (equilibrium entanglement density $\langle Z_k \rangle$ =17) with 705 chains in a canonical (NVT) ensemble. The entanglement network analysis has been performed by using the Z1 code developed by Kröger et al. [24, 25]. The reported quantities regarding the entangled network are averaged over the x-z plane along the flow gradient direction (y). To achieve steady state velocities, shear and first normal stresses, simulations up to 25 times the disengagement time of the system have been performed. In the simulations, the shear rate is non-dimensionalized by the longest relaxation time of the fluid at equilibrium, τ_{d0}, and expressed as Weissenburg number, $Wi = \dot{\gamma} \times \tau_{d0}$. Also, time, t, is scaled by the disengagement time of the entire system at the applied shear rate, i.e., τ_d. The disengagement time is calculated by fitting an exponential to the auto-correlation function of the chain unit end-to-end vector.

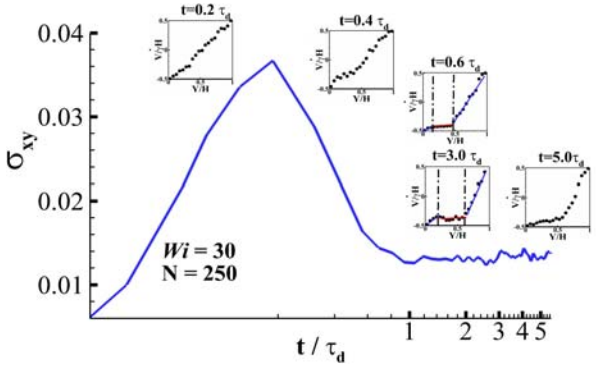

FIG 1. Steady shear banding observed in a step-strain experiment. The temporal evolution of velocity profiles is shown in the figure inset. This figure appeared in our previous publication [21]. It has been included to facilitate the discussion.

III. Macroscopic Results: Step-strain simulation

We begin by examining the characteristic response of a polymer melt to a step-strain start-up at Wi = 30 (Wi_R = 1.2, Weissenburg number based on the Rouse relaxation time; Rouse relaxation time scale, τ_R is estimated as follows: $\tau_R = \frac{\tau_{d0}}{3Z}$). The choice of the Wi has been motivated by the fact that this deformation rate is in the region where the steady shear stress is a slight decreasing function of shear rate (for more information, please refer to figure 1 in reference [21]). Also, a stress-overshoot exists under these conditions as shown in Figure 1. Chains, i.e., their corresponding primitive path are stretched and oriented at strains up to the stress overshoot, as they are mainly deformed affinely. Thus it is reasonable to assume that no inhomogeneity could arise prior to the time where the stress-overshoot is observed. This conclusion is corroborated by the evidence of linear velocity profile at the stress overshoot as depicted in the inset of Figure 1 as well as [19, 20]. However, after the stress-overshoot, at t = 0.4 τ_d, localized perturbations are observed in the velocity profile. These perturbations arise due to spatially-inhomogeneous chain entanglement density in the velocity gradient direction that leads to formation of the incipient shear banded structures at t = 0.6 τ_d [21]. Moreover, the slow (low shear rate) and fast (high shear rate) bands continue to develop (2 τ_d < t < 6 τ_d), i.e., the thickness of the slow band gradually increases until each band occupies nearly half of the box. At this point, the steady shear banded structure is realized.

IV. Macroscopic Results: Start-up of Shear Flow

To directly examine the influence of chain segmental stress relaxation (usually fast in the relaxation regime) and orientation relaxation times on formation of local inhomogeneities, a series of simulations have been performed by gradually increasing the imposed shear rate from zero to the final desired dimensionless deformation rate , i.e., Wi = 30. Specifically, three different ramp time (time taken for the shear rate to attain its steady state value) were studied, i.e., 2, 10 and 20 τ_d .

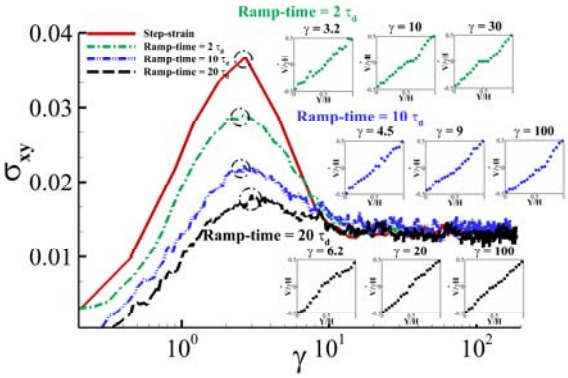

FIG 2. Influence of deformation rate ramp time on shear stress evolution as a function of strain; velocity profiles are shown in the inset.

Figure 2 depicts the shear stress evolution as a function of strain (time) for different ramp-times. The step-strain start-up shows a clear stress-overshoot. As the rate of deformation ramp-time is decreased, the stress-overshoot is diminished and eventually, at ramp-time = 20 τ_d, it almost disappears. As expected, the stress overshoot appears at strain units of approximately 2 and the steady stress shear stress values are identical for all ramp rates. However, the snap-shots of the velocity profile at different times as depicted in figure 1 and 2 insets are significantly different for different ramp-times. Specifically, robust shear banding is observed for the step-strain and fast start-up conditions (ramp-time $\leq 2\,\tau_d$), while for the slow ramp-times, i.e., 10 and $20\,\tau_d$, the linear velocity profile is maintained at all times. This finding clearly indicates that the temporal evolution of the velocity profile is a very sensitive function of the time scale over which the deformation rate is increased from zero to a given steady state value. Thus, shear banding is not a unique response of the flow at a specific shear rate even when the shear rate is in the region where the steady shear stress is a slight decreasing function of shear rate; rather its existence depends on the relaxation behavior of the entangled network as will be discussed herein. Specifically, a universal molecular criterion for the formation of inhomogeneity will be proposed henceforth.

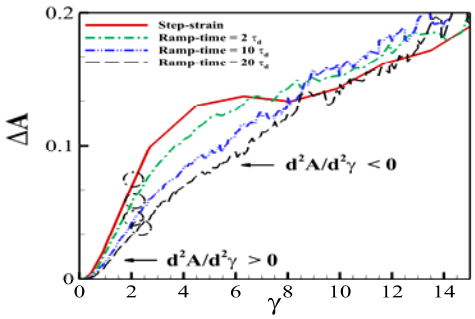

FIG 3. Free energy evolution as a function of strain for different ramp-times.

V. Microscopic Results: Free Energy Analysis and Chains' Relaxation Behavior

The Helmholtz free energy change per unit volume is evaluated as follows [26]: $\Delta A = -\frac{1}{2} < \left(Q + Q^{+}\right) : \sigma >$,

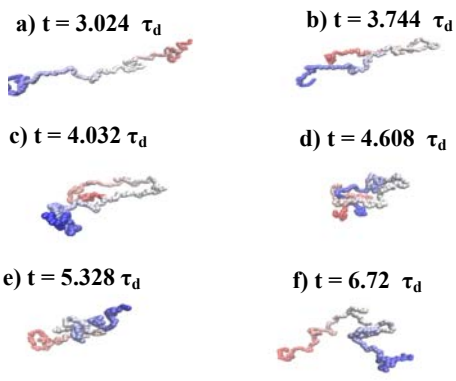

FIG 4. The chain rotation/retraction cycle of the step-strain start-up simulation at Wi = 30, N=250.

where $\left(Q+Q^{+}\right)/2$ denotes the strain tensor and σ is the total stress tensor with fluctuations. Figure 3, depicts the results of this analysis in kT units. Clearly, the free energy curvature is positive before the occurrence of the stress-overshoot at γ = 2. However, the curvature becomes negative for strain units larger than 2. Therefore, an inflection point in the free energy curve exists at the strain corresponding to the stress-overshoot. This inflection point in the free energy suggests flow instability in form of "local strain inhomogeneity" [4].

To understand the formation of local inhomogeneities, we have closely examined the chain dynamics during the stress relaxation process. The stress relaxes in two steps, first chains relax their tension via stretch relaxation which is quite fast and in the second process, chain segments relax their orientation from highly anisotropic flow induced configurations (stretched) to isotropic equilibrium like structures (coils). The latter process, namely, orientation relaxation is slow and it mainly occurs through a number of steps in a rotation/retraction cycle which leads to significant configurational diversity. A typical rotation/retraction cycle is shown in figure 4. During this cycle the chain retracts from a stretched configuration to a coil-like structure and expands once more to assume a stretched configuration. At *Wi=30*, the rotation/retraction cycle takes ~10 τ_d under step-strain conditions. Based on these observations, we propose that the large discrepancy between the stress and orientation relaxation time scales leads to local inhomogeneity in the entanglement network and hence inhomogeneous deformation. Specifically, the combination of flow induced chain disentanglement and insufficient time for orientation relaxation leads to inhomogeneous entanglement density and a commensurate local variations in fluid properties in the velocity gradient direction that cause a flow transition leading to formation of the incipient shear banded structure.

If the above mentioned molecular criterion for creation of local inhomogeneities is valid, one should be able to adjust the time scale for ramping up the deformation rate from zero to its steady state value such that chain stretch is delayed and orientation relaxation has sufficient time to occur, hence, obviating the formation of the incipient shear banded structure. Indeed, as deformation rate ramp-time is increased from 2 to 10, and finally to $20\,\tau_d$, the retraction/rotation time scale is reduced from 10.1 to 9.2, and $7.4\,\tau_d$, respectively. Thus, the ratio between the retraction/rotation time scale to deformation rate ramp-times of 2, 10 and $20\,\tau_d$, i.e., $\mathrm{MK}=\dfrac{\tau_{rot}}{\mathrm{ramp-time}}$ is decreased from 5.05 to 0.96, and 0.37, respectively. This decline in this ratio clearly shows that retraction/rotation cycle becomes more frequent and occurs globally prior to the system reaching its steady state value; hence, the main driving force for the formation of "local inhomogeneity" is suppressed and shear banding is eliminated.

To gain a more in-depth understanding of the interrelation between the chain longest relaxation time, local inhomogeneity and shear banding, we have thoroughly examined the primitive path segmental orientation distribution function at various deformation rate ramp times (see Figure 5). To quantify the segments that possess isotropic or anisotropic orientation, the following procedure has been used. The fraction of chains segments that have orientation angle between -45º and 45º with respect to the flow direction are labeled anisotropic, λ, hence, (1-λ) is the fraction of chain segments that have isotropic orientation angle, i.e., angles larger than 45º and smaller than -45º. Clearly, the isotropic fraction, (1-λ) increases as the ramp-time increases indicating more frequent chain retraction/rotation that allows more significant orientation relaxation to occur. On the other hand, in the anisotropic portion of the distribution function, the global maximum associated with the positive orientation angle declines and the local maximum corresponding to negative orientation angle grows as the ramp-time increases. It should be noted that the positive maximum value is associated with the fraction of the chain segments that are highly-oriented and stretched in the direction of the flow. While the negative maximum appears as a consequence of existence of a large number of folded configurations associated with the retraction/rotation cycle (see Figure 4-b, c, e). Thus, the significant drop in the positive maximum peak and considerable growth of the negative maximum peak clearly

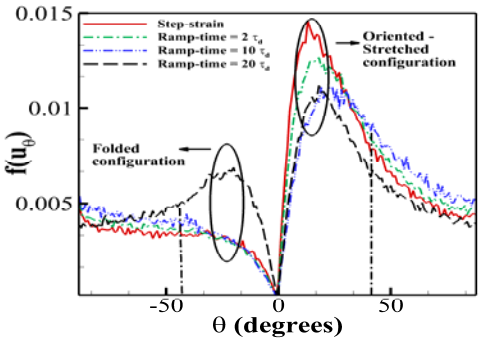

indicates that as the ramp time is increased, the rotation/retraction cycle leads to global orientation relaxation (in the entire simulation box) as opposed to local orientation relaxation as is the case for fast start-up flows.

FIG 5. Primitive path segmental orientation distribution at various ramp times.

The intricate relation between the relaxation time scale, chain disentanglement and formation of local inhomogeneity can also be quantified by examining the average time for flow induced chain disentanglement as a function of deformation rate ramp time (See Figure 6).

Clearly at large ramp-time = 10, 20 τ_d (r < 1), the flow induced chain disentanglement occurs at a commensurate time scale (see Figure 6a) as the retraction/rotation process leading to a homogeneous entanglement density along the

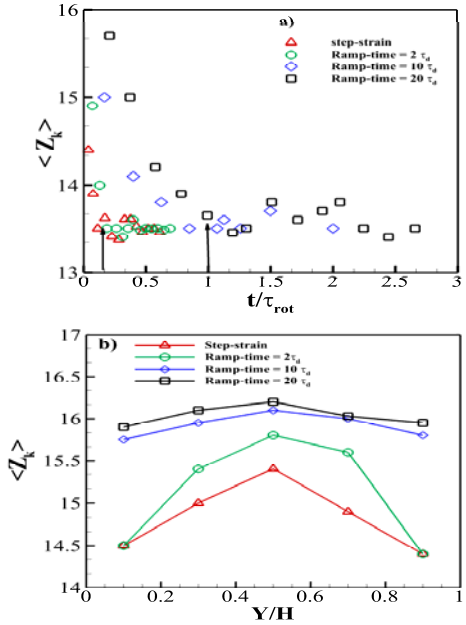

FIG 6. Average number of entanglements a) as a function of time and b) along the velocity gradient direction Y, at different ramp times. Y is scaled by the simulation box length, H.

velocity gradient direction (see Figure 6-b). However, in the case of fast start-up, i.e., step-strain and ramp-time over 2 τ_d (r > 1), the chain disentanglement occurs much faster than the time scale associated with the retraction/rotation time scale; hence, giving rise to a locally inhomogeneous entanglement density along the velocity gradient direction. This in turn, gives rise to a localized jump in fluid viscosity and normal stresses that leads to shear banding (please see reference [21]).

VI. Local Process of Shear Banding Formation

The local perturbations are observed for the first time at t = 0.4 τ_d (see velocity profiles in the inset of Figure 1). In order to study the origin of this perturbations, we have investigated the entanglement network behavior at the step-strain and slow (ramp-time= 20 τ_d) start-up of *Wi*=30 at 0.25 $\tau_d \le t \le 0.4\ \tau_d$ (the stress-overshoot occurs at t = 0.2 τ_d). Various number of equal sub-volumes of the simulation box have been examined. Here the three main regions labeled as lower, middle and upper regions are discussed since they provide more meaningful statistical results.

The movie (primitive_path.pm4) shows the chains' primitive path evolution for the step strain simulation as a function of time between $0.25\tau_d \le t \le 0.4\tau_d$, i.e., before the occurrence of incipient shear banding at t = 0.6 τ_d. Beads indicate the entanglement defined and detected by Z1 code and the lines are primitive path segments. It is evident that the chain primitive path movement in the upper and lower regions of the box are less restricted and they disengage from the original tube much faster as compared to the chains in the middle region. Chain disengagement can be triggered by "higher kinetic energy" in the boundary regions due to the Lees-Edwards boundary condition providing higher velocities towards the box ends. Thus, the chains in the boundary regions relax their orientation and "chain

disentanglement rate" is larger in the aforementioned regions while chains in the middle of the box cannot relax their orientation as rapidly as the higher kinetic energy region. Hence, the local criterion for the formation of inhomogeneity is provided at some time after stress overshoot when the chains in the two adjacent regions disentangle and relax their orientation on a different time scale, therefore inhomogeneity forms in deformation at the interface between the two aforementioned regions. To determine the location of inhomogeneity or the interface, we have looked at the number of entanglement points (different from number of entanglement per chain; time averaged over $0.25\ \tau_d \le t \le 0.4\ \tau_d$) over the X-Z and X-Y plane. The number of entanglement points in each cell are counted. It is clear from the X-Y contour shown in Figure 7-(a) that asymmetry in the entanglement distribution exists at y = 8 and 32 r_c (box length in y dimension is 42.0 r_c). These two positions correspond to the locations in Figure 1 velocity profile inset at t = 0.4 τ_d where velocity perturbations are observed. The entanglement distribution for ramp-time = 20 τ_d is shown in Figure 7-(b) averaged over $3 < \gamma < 5$. The gradient of entanglement along the y direction in the case of ramp-time = 20 τ_d is smaller than the step-strain case as the dense contour lines suggest. The data points in Figure 7-(a,b) indicate the position and level of each contour. We have extremely examined various planes in the vicinity of asymmetry in entanglement distribution, and have found that $\frac{\Delta Z}{\Delta Y}$ for the case of step-strain is larger than 3 and for the case of slow start-up (ramp-time = 20 τ_d) is smaller than 2. This point indicates that discontinuity in the number of entanglement should reach a critical value for inhomogeneity in deformation to occur.

The X-Z entanglement contours for different regions (upper, lower and middle) of the box show similar behavior (see Figure 8). However, the number of entanglements is different in each region. Overall, the number of entanglements in the core of each region is highest and disengagement occurs from the tube ends. The orientation relaxation occurs at higher rate in regions close to the boundaries and thus a discontinuity in chain disentanglement appears in adjacent high and low kinetic energy regions and an interface between them is formed. Eventually, the lower and upper regions form the fast bands and the middle region becomes the slow band. If we consider the position of the interface at y = δ (the distance from the center of the box), δ is not randomly determined. Instead it is located somewhere between the boundaries

and middle of the box which is a function of chain length (viscosity and elasticity), and shear rate in the stress relaxation regime. The interface is eventually stabilized when the viscous and elastic forces are balanced. It should be mentioned that in the entanglement network analysis (Figures 7 and 8), the central box and the adjacent boxes are also available to clearly count the number of entanglement points, the central box dimension is $100\times42\times42\,(r_c^3)$.

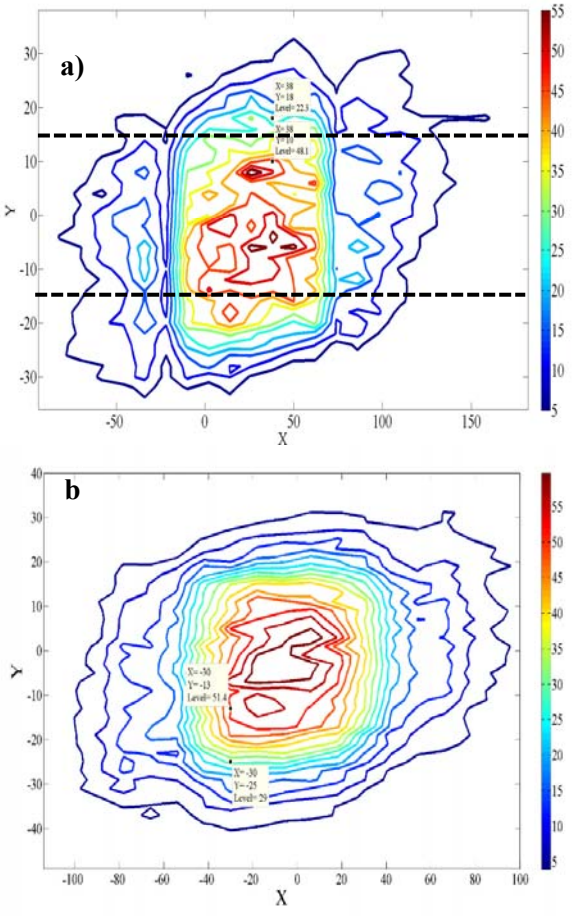

Figure 7. a) Step-strain entanglement distribution in X-Y plane, b) Contour plot of number of entanglements at ramp-speed =20 τ_d. The dashed lines indicate the interface between the adjacent regions. $\frac{\Delta Z}{\Delta Y}$ > 3 and < 2 for step strain and ramp-speed =20 τ_d.

VII. Conclusion

In conclusion, we have demonstrated that shear banding is not a unique response of entangled polymeric fluids to a specific shear rate. Moreover, a molecular picture for the interrelation between longest orientation relaxation time, local inhomogeneities, and shear banding has been proposed and corroborated. Moreover, the local process for the formation of shear bands is discussed in terms of chain disentanglement rates reaching a critical value as a result of different relaxation processes. Overall, if the orientation and stretch relaxation time scales differ significantly, the orientation relaxation occurs "locally", thus the chain disentanglement rate becomes different in the adjacent regions, hence an interface and consequently inhomogeneous deformation is observed. Finally, our findings regarding the influence of deformation ramp time on shear banding is supported by continuum linear stability analysis of Moorcroft and Fielding [18] as well as experimental findings of Wang and coworkers with monodisperse entangled DNA [7] where a ramp-time of $12.82\,\tau_{d0}$ was used to eliminate shear banding in a cone-plate rheometer.

The authors would like to acknowledge the National Science Foundation (EPS-1004083) as well as the University of Tennessee and Oak Ridge National Laboratory Joint Institute for Computational Sciences for the support of this work.

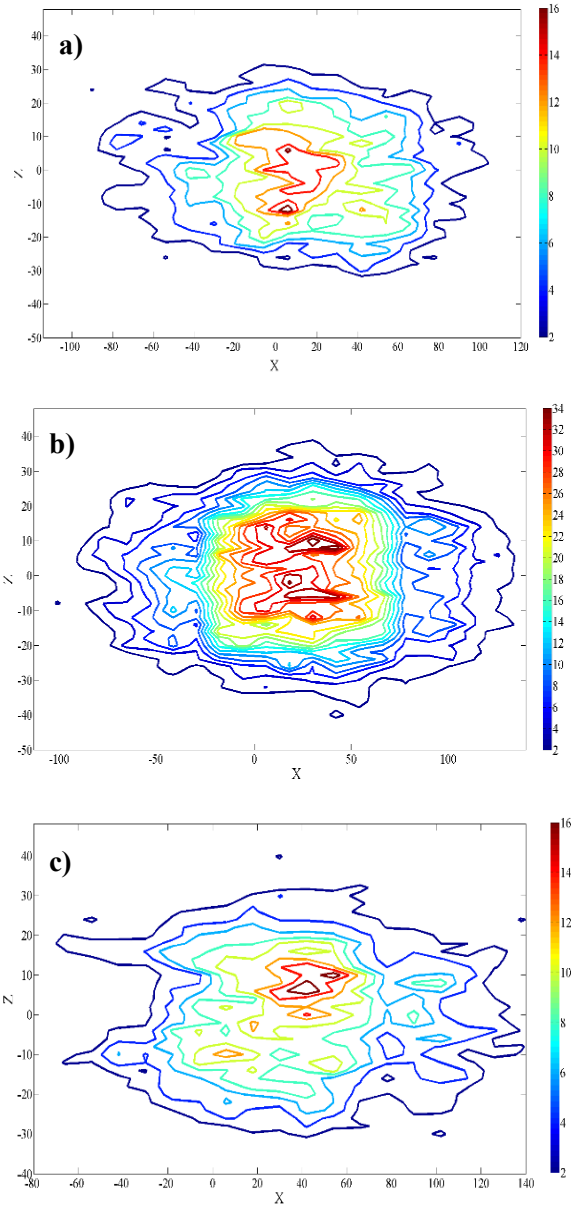

Figure 8. Number of entanglement points in the X-Z plane in (a) lower region (future fast band) (b) middle region (future slow band) (c) upper region (future fast band).

References

[1] M.E. Cates, Nonlinear viscoelasticity of wormlike micelles (and other reversibly breakable polymers), The Journal of Physical Chemistry **94**, 371 (1990).

[2] N.A. Spenley, M.E. Cates, and T.C.B. McLeish, Nonlinear rheology of wormlike micelles, Physical Review Lett. **71**, 939 (1993).

[3] P. Tapadia and S.-Q. Wang, Direct Visualization of Continuous Simple Shear in Non-Newtonian Polymeric Fluids, Physical Review Lett. 2006. **96**, 016001 (2006).

[4] G. Marrucci and N. Grizzuti, The Free Energy Function of the Doi-Edwards Theory: Analysis of the Instabilities in Stress Relaxation, Journal of Rheology **27**, 433 (1983).

[5] M. Doi and S.F. Edwards, Dynamics of concentrated polymer systems. Part 4.-Rheological properties, Journal of the Chemical Society, Faraday Transactions 2: Molecular and Chemical Physics **75**, 38 (1979).

[6] P. E. Boukany, Y.T. Hu, and S.-Q. Wang, Observations of Wall Slip and Shear Banding in an Entangled DNA Solution, Macromolecules **41**, 2644 (2008).

[7] P.E. Boukany and S.-Q. Wang, Shear Banding or Not in Entangled DNA Solutions, Macromolecules **43**, 6950 (2010).

[8] S. Ravindranath and S.-Q. Wang, Large amplitude oscillatory shear behavior of entangled polymer solutions: Particle tracking velocimetric investigation, Journal of Rheology **52**, 341 (2008).

[9] S. Ravindranath and S.-Q. Wang, What Are the Origins of Stress Relaxation Behaviors in Step Shear of Entangled Polymer Solutions? Macromolecules **40**, 8031 (2007).

[10] P. Tapadia, S. Ravindranath, and S.-Q. Wang, Banding in Entangled Polymer Fluids under Oscillatory Shearing, Physical Review Lett. **96**, 196001 (2006).

[11] C. Sui and G. McKenna, Instability of entangled polymers in cone and plate rheometry, Rheologica Acta **46**, 877 (2007).

[12] J. M. Adams and P.D. Olmsted, Nonmonotonic Models are Not Necessary to Obtain Shear Banding Phenomena in Entangled Polymer Solutions, Physical Review Lett. **102**, 067801 (2009).

[13] S. M. Fielding and P.D. Olmsted, Kinetics of the shear banding instability in startup flows, Physical Review E **68**, 036313 (2003).

[14] P. Olmsted, Perspectives on shear banding in complex fluids, Rheologica Acta **47**, 283 (2008).

[15] P.D. Olmsted, O. Radulescu, and C.-Y.D. Lu, Johnson–Segalman model with a diffusion term in cylindrical Couette flow, Journal of Rheology **44**, 257 (2000).

[16] A. E. Likhtman and R.S. Graham, Simple constitutive equation for linear polymer melts derived from molecular theory: Rolie–Poly equation, Journal of Non-Newtonian Fluid Mechanics **114**, 1 (2003).

[17] J.M. Adams, S.M. Fielding, and P.D. Olmsted, Transient shear banding in entangled polymers: A study using the Rolie-Poly model, Journal of Rheology **55**, 1007 (2011).

[18] R. L. Moorcroft and S.M. Fielding, Criteria for Shear Banding in Time-Dependent Flows of Complex Fluids, Physical Review Lett. **110**, 086001 (2013).

[19] M. Cromer, et al., Shear banding in polymer solutions, Physics of Fluids **25**, 051703 (2013).

[20] F. A. Morrison and R.G. Larson, A study of shear-stress relaxation anomalies in binary mixtures of monodisperse polystyrenes, Journal of Polymer Science Part B: Polymer Physics **30**, 943 (1992).
[21] M. Mohagheghi and B. Khomami, Molecular Processes Leading to Shear Banding in Well Entangled Polymeric Melts, ACS Macro Lett. **4**, 684 (2015).
[22] P. Nikunen, I. Vattulainen, and M. Karttunen, Reptational dynamics in dissipative particle dynamics simulations of polymer melts, Physical Review E **75**, 036713 (2007).
[23] A.W. Lees and S.F. Edwards, The computer study of transport processes under extreme conditions, Journal of Physics C: Solid State Physics **5**, 192 (1972).
[24] M. Kröger, Shortest multiple disconnected path for the analysis of entanglements in two- and three-dimensional polymeric systems, Computer Physics Communications **168**, 209 (2005).
[25] S. Shanbhag and M. Kröger, Primitive Path Networks Generated by Annealing and Geometrical Methods: Insights into Differences. Macromolecules **40**, 2897 (2007).
[26] M. Doi and S.F. Edwards, Dynamics of rod-like macromolecules in concentrated solution. Part 2, Journal of the Chemical Society, Faraday Transactions 2: Molecular and Chemical Physics **74**, 918 (1978).